



Audio Engineering Society
Convention Paper 9596

Presented at the 140th Convention
2016 June 4–7, Paris, France

This convention paper was selected based on a submitted abstract and 750-word precis that have been peer reviewed by at least two qualified anonymous reviewers. The complete manuscript was not peer reviewed. This convention paper has been reproduced from the author's advance manuscript without editing, corrections, or consideration by the Review Board. The AES takes no responsibility for the contents. This paper is available in the AES E-Library (<http://www.aes.org/e-lib>), all rights reserved. Reproduction of this paper, or any portion thereof, is not permitted without direct permission from the Journal of the Audio Engineering Society.

Local Wave Field Synthesis by Spatial Band-limitation in the Circular/Spherical Harmonics Domain

Nara Hahn, Fiete Winter, and Sascha Spors

Institute of Communications Engineering, University of Rostock, Germany

Correspondence should be addressed to Nara Hahn (nara.hahn@uni-rostock.de)

ABSTRACT

The achievable accuracy of sound field synthesis (SFS) techniques, such as Wave Field Synthesis (WFS), is mainly limited in practice due to the limited loudspeaker density. Above the so called spatial aliasing frequency, considerable artifacts are introduced in the synthesized sound field. In local SFS, the accuracy within a local listening area is increased at the cost of degradations outside. In this paper a new approach for local WFS is proposed. The WFS driving functions are computed based on an order-limited harmonics expansion of the target sound field. A local listening area is created around the shifted expansion center where the synthesized sound field exhibits higher accuracy. The size of the local area is controlled by the expansion order of the driving function. The derivations of 2D, 3D and 2.5D driving functions are given, and the synthesized sound fields are evaluated by numerical simulations.

1 Introduction

Sound field synthesis (SFS) is a spatial sound reproduction technique where a desired sound field is physically reconstructed by a loudspeaker array. The loudspeakers, termed secondary sources, are driven individually in such a way that the superposition of the reproduced sound fields approaches the target sound field. Two well established SFS methods are Wave Field Synthesis (WFS) and near-field compensated higher-order Ambisonics (NFC-HOA) [1, 2, 3, 4]. Theoretically, a continuous distribution of secondary sources is required for a perfect synthesis. In practice, only a finite number of secondary sources can be placed at dis-

crete positions. The spatial discretization results in spatial aliasing and a prominent artifacts are introduced in the synthesized sound field. In general, the amount of artifacts depends on the number and the distribution of the secondary sources, as well as on the virtual source position and the listener position [5].

Instead of considering the entire listening area, local SFS techniques aim at increasing the physical accuracy inside a predetermined local listening area [6, 7, 8, 9]. This is typically achieved at the cost of stronger artifacts outside the local area. In NFC-HOA, for instance, the local listening area can be shifted by translating the expansion center to a target listening position [7]. The size of

the local area is controlled by the spatial bandwidth (circular/spherical harmonic order) of the driving function. Some extensions of local NFC-HOA were introduced and investigated in [10]. For local WFS, two approaches are known so far. In [8], a virtual loudspeaker array is created using focused sources. By choosing a dense distribution of virtual loudspeakers, the spatial aliasing frequency is increased and a better performance can be achieved in the local area. The second local WFS method proposed in [9] employs the equivalent scattering approach [11]. Here, the boundary of the local listening area is assumed to be a sound-soft scatterer. For a given incident field (target field), the local WFS driving functions are computed based on the sound field scattered by the virtual boundary.

In this paper, an alternative method for local WFS is presented. Unlike the above mentioned local WFS methods, no explicit boundary is considered. It rather exploits the properties of a spatially band-limited sound field which exhibits higher accuracy around the expansion center. Similar to (local) NFC-HOA, the desired sound field is described as a circular/spherical harmonics expansion with a limited order. The local WFS driving functions are obtained by (i) computing the directional gradient at each secondary source position and (ii) applying a spatial window that activates only the secondary sources illuminated by the virtual source [12]. Since the derivatives of the spherical/circular harmonics and the Bessel functions are known, analytic driving functions can be derived for typical virtual sources, e.g. plane waves and point sources.

The derivation of WFS driving function based on a harmonics representation was also presented in [13], but in a slightly different context. It was assumed that the sound field is captured e.g. by a spherical microphone array and thus the direction of arrival of the source is unknown. The captured sound field is thus decomposed into plane waves so that the selection of active secondary sources becomes more convenient. In this paper, it is assumed that the position of the virtual source is known. The driving functions are thus computed directly from the harmonics coefficients. The focus is on increasing the local accuracy of the synthesized sound field.

It is worth noting that the presented derivations are mathematically similar to the works in [14], [15] and [16]. In the latter studies, the source directivity is represented by spherical/circular harmonics. The center of expansion is placed outside the listening area, and thus the sound field is expressed as an exterior expansion using singular basis functions. The expansion order depends on the complexity of the directivity. In this paper, on the contrary, the expansion center has to be located within the listening area, and the sound field is described by an interior expansion using regular basis functions. The expansion order of the sound field is determined by the size of the local area.

This paper is structured as follows. Notational and mathematical conventions are defined in Sec. 1.1. The concept of local SFS are reviewed and the local WFS driving functions are derived in Sec. 2. The proposed method is evaluated by numerical simulations and the properties of the synthesized sound field are discussed in Sec. 3.

1.1 Nomenclature and Mathematical Preliminaries

In this paper, the complex sound pressure at position \mathbf{x} is denoted by uppercase $S(\mathbf{x}, \omega)$ where the radial frequency ω is related to the temporal frequency by $\omega = 2\pi f$. The complex unit i is defined as $i^2 = -1$, and the speed of sound is denoted by c and assumed to be constant.

The cylindrical coordinates (ρ, φ, z) is related to its Cartesian coordinates (x, y, z) by

$$\begin{aligned}x &= \rho \cos \varphi \\y &= \rho \sin \varphi \\z &= z\end{aligned}$$

where ρ denotes the radial distance from the z -axis and φ the polar angle from the x -axis. The spherical coordinates (r, θ, ϕ) is related to the Cartesian coordinates by

$$\begin{aligned}x &= r \cos \phi \sin \theta \\y &= r \sin \phi \sin \theta \\z &= r \cos \phi\end{aligned}$$

where r denotes the radial distance from the origin, ϕ the azimuth angle from the x -axis, and θ the colatitude angle measured from the z -axis.

Within a source-free region, a propagating sound field can be represented as a combination of the regular basis solutions of the wave equation. A two-dimensional homogeneous sound field independent to the z -coordinate can be expanded with respect to a line ($\rho = \rho_c, \varphi = \varphi_c$) parallel to the z -axis [17, Eq. (4.49)]

$$S(\rho', \varphi', \omega) = \sum_{\mu=-\infty}^{\infty} \hat{S}_{\mu}(\omega) J_{\mu}(\frac{\omega}{c} \rho') e^{i\mu\varphi'} \quad (1)$$

where $J_{\mu}(\frac{\omega}{c} \rho')$ denotes the Bessel function of the first kind of order μ , $e^{i\mu\varphi'}$ the μ -th circular harmonic and $\hat{S}_{\mu}(\omega)$ the corresponding expansion coefficient. The primed variables (ρ', φ') denote the radial distance and the polar angle from the line of expansion, respectively.

A three-dimensional homogeneous sound field can be represented as a spherical harmonics expansion [17, Eq. (6.140)]

$$S(\mathbf{x} - \mathbf{x}_c, \omega) = \sum_{n=0}^{\infty} \sum_{m=-n}^n \check{S}_n^m(\omega) j_n(\frac{\omega}{c} r') Y_n^m(\theta', \phi') \quad (2)$$

where $j_n(\frac{\omega}{c} r')$ denotes the spherical Bessel function of the first kind of order n , $Y_n^m(\theta', \phi')$ the spherical harmonic, and $\check{S}_n^m(\omega)$ the corresponding expansion coefficient. The spherical harmonic is defined as

$$Y_n^m(\theta', \phi') = \sqrt{\frac{2n+1}{4\pi} \frac{(n-m)!}{(n+m)!}} P_n^m(\cos \theta') e^{im\phi'} \quad (3)$$

with $P_n^m(\cdot)$ denoting the associated Legendre polynomial. The primed variables are defined as $\mathbf{x} - \mathbf{x}_c = (r', \theta', \phi')$.

Inside a cylindrical ($\rho' < R$) or spherical ($r' < R$) region, the sound field can be approximated by a finite number of harmonics with bounded error [18]. Both for (1) and (2), the required order is typically approximated by $\mathcal{N} \equiv \lceil \frac{\omega}{c} R \rceil$ where $\lceil \cdot \rceil$ denotes the ceiling function. The corresponding number of harmonics is $2\mathcal{N} + 1$ for the circular harmonics expansion

$$S_{\mathcal{N}}(\mathbf{x} - \mathbf{x}_c, \omega) = \sum_{\mu=-\mathcal{N}}^{\mathcal{N}} \hat{S}_{\mu}(\omega) J_{\mu}(\frac{\omega}{c} \rho') e^{i\mu\varphi'} \quad (4)$$

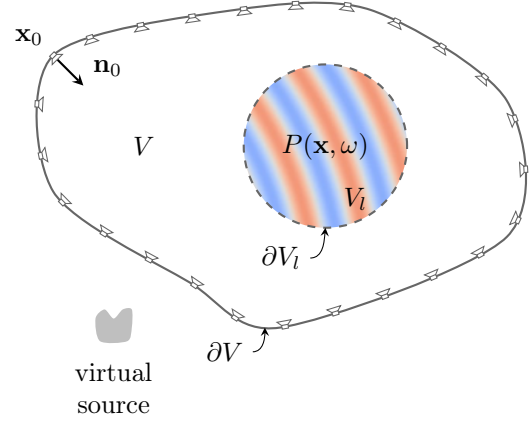


Fig. 1: Local sound field synthesis. The desired sound field is synthesized inside the local listening area V_l by using the secondary sources distributed on ∂V .

and $(\mathcal{N} + 1)^2$ for the spherical harmonics expansion

$$S_{\mathcal{N}}(\mathbf{x} - \mathbf{x}_c, \omega) = \sum_{n=0}^{\mathcal{N}} \sum_{m=-n}^n \check{S}_n^m(\omega) j_n(\frac{\omega}{c} r') Y_n^m(\theta', \phi'). \quad (5)$$

In the remainder, \mathcal{N} is frequently referred to as the spatial bandwidth of a sound field.

For convenience, the coordinate system is always translated by $-\mathbf{x}_c$ so that the expansion center coincides with the origin of the coordinate system. Thus, $(\rho', \varphi', z') = (\rho, \varphi, z)$ and $(r', \theta', \phi') = (r, \theta, \phi)$.

2 Local WFS

2.1 Problem Statement

As illustrated in Fig. 1, local SFS techniques aim at the physical reconstruction of a desired sound field $S(\mathbf{x}, \omega)$ within a local region $\mathbf{x} \in V_l$ by using multiple loudspeakers distributed on $\mathbf{x}_0 \in \partial V$. The synthesized sound field $P(\mathbf{x}, \omega)$ is a superposition of the sound fields emitted by the individual secondary sources. For a continuous secondary source distribution, the reproduced sound field reads

$$P(\mathbf{x}, \omega) = \int_{\partial V} D(\mathbf{x}_0, \omega) G(\mathbf{x} - \mathbf{x}_0, \omega) dA_0 \quad (6)$$

where $D(\mathbf{x}_0, \omega)$ denotes the driving function of the secondary source at \mathbf{x}_0 and $G(\mathbf{x} - \mathbf{x}_0, \omega)$ the Green's function characterizing the spatio-temporal transfer function of the secondary sources. Equation (6) is either a surface integral or a contour integral depending on the dimensionality of the problem. The goal is to find $D(\mathbf{x}_0, \omega)$ that satisfies $P(\mathbf{x}, \omega) = S(\mathbf{x}, \omega)$ for $\mathbf{x} \in V_l$. If V_l coincides with V it becomes a conventional SFS problem.

2.2 Driving Function

WFS constitutes a high-frequency/far-field solution of (6) based on the Kirchhoff-Helmholtz integral equation. A detailed theoretical introduction on WFS can be found in [2]. The WFS driving function is given as the directional gradient of the sound field evaluated at the secondary source position $\mathbf{x}_0 \in \partial V$,

$$D(\mathbf{x}_0, \omega) = -2a(\mathbf{x}_0) \langle \nabla S(\mathbf{x}, \omega)|_{\mathbf{x}=\mathbf{x}_0}, \mathbf{n}_0 \rangle \quad (7)$$

where \mathbf{n}_0 denotes the normal vector on ∂V pointing inward, and $\langle \cdot, \cdot \rangle$ the scalar product of two vectors. The window function $a(\mathbf{x}_0)$ activates only the secondary sources where the inner product of the propagation direction and \mathbf{n}_0 is positive [12]. In the following derivation, $a(\mathbf{x}_0)$ is omitted for convenience. The gradient ∇ is defined as

$$\nabla_{\text{Cart}} \equiv \hat{\mathbf{e}}_x \frac{\partial}{\partial x} + \hat{\mathbf{e}}_y \frac{\partial}{\partial y} + \hat{\mathbf{e}}_z \frac{\partial}{\partial z} \quad (8)$$

in Cartesian coordinates,

$$\nabla_{\text{cyl}} \equiv \hat{\mathbf{e}}_\rho \frac{\partial}{\partial \rho} + \hat{\mathbf{e}}_\varphi \frac{1}{\rho} \frac{\partial}{\partial \varphi} + \hat{\mathbf{e}}_z \frac{\partial}{\partial z} \quad (9)$$

in cylindrical coordinates, and

$$\nabla_{\text{sph}} \equiv \hat{\mathbf{e}}_r \frac{\partial}{\partial r} + \hat{\mathbf{e}}_\theta \frac{1}{r} \frac{\partial}{\partial \theta} + \hat{\mathbf{e}}_\phi \frac{1}{r \sin \theta} \frac{\partial}{\partial \phi} \quad (10)$$

in spherical coordinates where $\hat{\mathbf{e}}$ denotes the respective unit vector.

2.3 Local WFS by Spatial Band-limitation

In this paper, the sound field in the local listening area is controlled by limiting the spatial bandwidth of $S(\mathbf{x}, \omega)$ in the circular/spherical harmonics domain. Due to the properties of a spatially band-limited sound field discussed in Sec. 1.1, only

circular/spherical local listening area is considered. The virtual sound field $S(\mathbf{x}, \omega)$ is expanded with respect to the center of the local area V_l . If a local area with a radius of R_l is desired, the spatial bandwidth is limited by $\mathcal{N} = \lceil \frac{\omega}{c} R_l \rceil$. The larger the spatial bandwidth, the bigger the local listening area.

In the following, WFS driving functions are derived for different secondary source distributions and dimensionalities of the virtual sound field. The driving functions are summarized in Table. 1.

2.4 2D Local WFS Driving Function

Two-dimensional (2D) WFS is first considered. Here a height-invariant sound field is synthesized by using secondary line sources having a 2D distribution, e.g. linear or circular array. The secondary line sources are aligned perpendicular to the horizontal plane, i.e. parallel to the z -axis. The spatio-temporal response of a line source is given by the 2D Green's function [17, Eq. (8.51)]

$$G_{2D}(\mathbf{x} - \mathbf{x}_0, \omega) = -\frac{i}{4} H_0^{(2)}\left(\frac{\omega}{c} \|\mathbf{x} - \mathbf{x}_0\|\right) \quad (11)$$

where $H_0^{(2)}(\cdot)$ denotes the 0-th Hankel function of the second kind.

The virtual sound field is represented by a circular harmonics expansion (4). To derive the driving function by (7), the individual components of the directional gradient are computed [19],

$$\begin{aligned} \frac{\partial}{\partial \rho} S(\mathbf{x}, \omega) = & \\ & \sum_{\mu=-\mathcal{N}}^{\mathcal{N}} \hat{S}_\mu(\omega) \frac{\omega}{2c} [J_{\mu-1}\left(\frac{\omega}{c} \rho\right) - J_{\mu+1}\left(\frac{\omega}{c} \rho\right)] e^{i\mu\varphi} \end{aligned} \quad (12)$$

and

$$\frac{\partial}{\partial \varphi} S(\mathbf{x}, \omega) = \sum_{\mu=-\mathcal{N}}^{\mathcal{N}} \hat{S}_\mu(\omega) J_\mu\left(\frac{\omega}{c} \rho\right) (i\mu) e^{i\mu\varphi} \quad (13)$$

while

$$\frac{\partial}{\partial z} S(\mathbf{x}, \omega) = 0 \quad (14)$$

due to the height invariance. In (12), the recurrence relation of $J_\mu(\cdot)$ is exploited [19, Eq. (9.1.27)]. The directional gradient is computed by substituting (12), (13) and (14) into (9). The 2D WFS

driving function is then obtained by substituting (9) into (7)

$$D_{2D}(\mathbf{x}_0, \omega) = -2 \sum_{\mu=-N}^N \check{S}_\mu(\omega) e^{i\mu\varphi_0} \times \left[\langle \hat{\mathbf{e}}_r, \mathbf{n}_0 \rangle \frac{\omega}{2c} \left\{ J_{\mu-1}\left(\frac{\omega}{c}\rho_0\right) - J_{\mu+1}\left(\frac{\omega}{c}\rho_0\right) \right\} + \langle \hat{\mathbf{e}}_\varphi, \mathbf{n}_0 \rangle i\mu J_\mu\left(\frac{\omega}{c}\rho_0\right) \right]. \quad (15)$$

Although not considered in this paper, the large argument approximation of $J_\mu(\cdot)$ may be considered to reduce the computational complexity [19, Eq. (9.2.1)].

2.5 3D Driving Function

In three-dimensional (3D) WFS, a virtual sound field is synthesized by using secondary point sources that have a 3D distribution, e.g. planar or spherical array. The spatio-temporal transfer function of a point source is given as the 3D Green's function [17, Eq. (8.41)],

$$G_{3D}(\mathbf{x} - \mathbf{x}_0, \omega) = \frac{1}{4\pi} \frac{e^{-i\frac{\omega}{c}\|\mathbf{x}-\mathbf{x}_0\|}}{\|\mathbf{x} - \mathbf{x}_0\|}. \quad (16)$$

The virtual sound field exhibits three-dimensional properties and can be represented by its spherical harmonics expansion. The individual components of the directional gradient in (10) are

$$\frac{\partial}{\partial r} S(\mathbf{x}, \omega) = \sum_{n=0}^N \sum_{m=-n}^n \check{S}_n^m(\omega) \times \frac{\omega}{c} \frac{n j_{n-1}\left(\frac{\omega}{c}r\right) - (n+1) j_{n+1}\left(\frac{\omega}{c}r\right)}{2n+1} Y_n^m(\theta, \phi), \quad (17)$$

$$\frac{\partial}{\partial \theta} S(\mathbf{x}, \omega) = \sum_{n=0}^N \sum_{m=-n}^n \check{S}_n^m(\omega) j_n\left(\frac{\omega}{c}r\right) \times \frac{-1}{\sin^2 \theta} \left[(n+1) \cos \theta Y_n^m(\theta, \phi) - \sqrt{\frac{2n+1}{2n+3}} \left((n+1)^2 - m^2 \right) Y_{n+1}^m(\theta, \phi) \right] \quad (18)$$

and

$$\frac{\partial}{\partial \phi} S(\mathbf{x}, \omega) = \sum_{n=0}^N \sum_{m=-n}^n \check{S}_n^m(\omega) j_n\left(\frac{\omega}{c}r\right) (im) Y_n^m(\theta, \phi). \quad (19)$$

In (17) the recurrence relation of $j_n(\cdot)$ is exploited [19, Eq. (10.1.20)], and in (18) the recurrence relation of $P_n^m(\cdot)$ is used [19, Eq. (8.5.3) and (8.5.4)]. The directional gradient is computed by substituting (17), (18) and (19) into (10). The WFS driving function is computed by substituting (10) into (7). The resulting driving function (25) is listed in Table 1.

Obviously, a SFS system with a 3D secondary source distribution is capable of synthesizing a 2D sound field that is represented by $\check{S}_\mu(\omega)$. One may directly use the driving functions derived in (15). If necessary, $\check{S}_\mu(\omega)$ can be converted to $\check{S}_n^m(\omega)$ by using the relation in [20, Eq. (14)] and plugging it into the 3D driving function (25).

2.6 2.5D Driving Function I – $\check{S}_\mu(\omega)$

In practice, 2D WFS is infeasible since secondary line sources are not available. A typical loudspeaker exhibits a point-source-like characteristic. Therefore a 2D distribution (e.g. linear or circular array) of secondary point sources is often used in SFS systems. This constitutes a dimensionality mismatch and the 2D driving functions in (15) cannot be used directly.

According to the large argument approximation of $H_m^{(2)}(\cdot)$ [19, Eq. (9.2.4)], the 2D Green's function is related to the 3D Green's function by

$$G_{2D}(\mathbf{x} - \mathbf{x}_0, \omega) \approx \sqrt{\frac{2\pi\|\mathbf{x}-\mathbf{x}_0\|}{i\frac{\omega}{c}}} G_{3D}(\mathbf{x} - \mathbf{x}_0, \omega) \quad (20)$$

for $\frac{\omega}{c}\|\mathbf{x} - \mathbf{x}_0\| \gg 1$. The latter is also known as the stationary phase approximation. If (20) is plugged into (6), the synthesis equation reads

$$P(\mathbf{x}, \omega) = \int_{\partial V} D_{2D}(\mathbf{x}_0, \omega) \sqrt{\frac{2\pi\|\mathbf{x}-\mathbf{x}_0\|}{i\frac{\omega}{c}}} G_{3D}(\mathbf{x} - \mathbf{x}_0, \omega) dA_0. \quad (21)$$

The above equation can be interpreted as SFS where secondary point sources are driven by the 2.5D driving function

$$D_{2.5D}(\mathbf{x}_0, \omega) = \sqrt{\frac{2\pi\|\mathbf{x}-\mathbf{x}_0\|}{i\frac{\omega}{c}}} D_{2D}(\mathbf{x}_0, \omega). \quad (22)$$

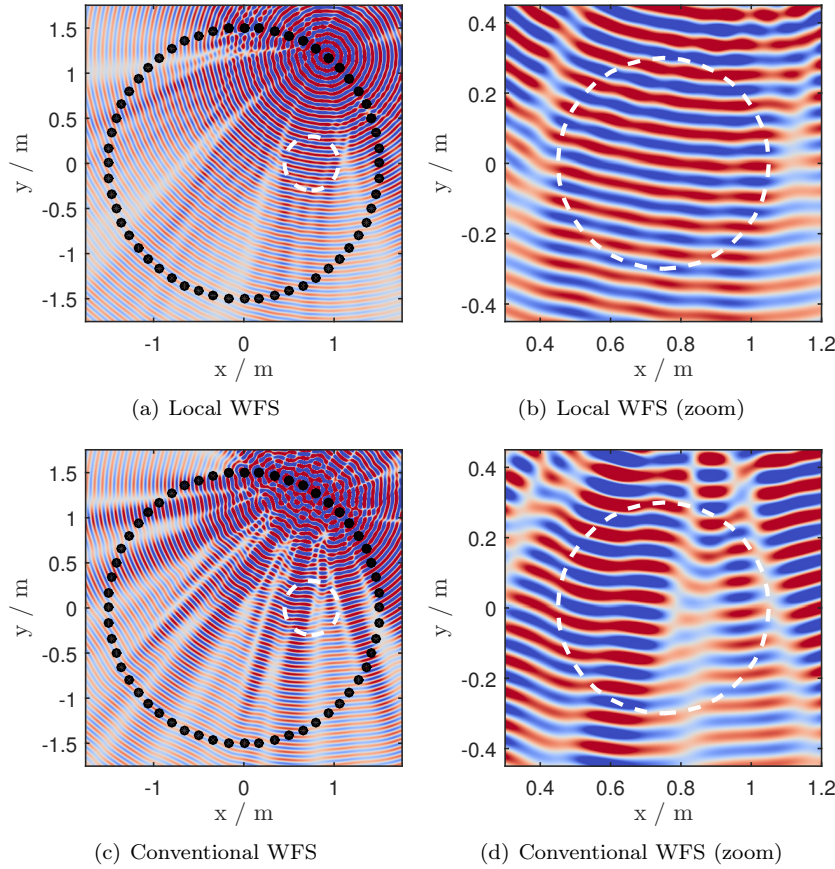


Fig. 2: Virtual point source at $(1, 1.7, 0)$ with frequency of $f = 4$ kHz was synthesized by using a circular loudspeaker array (56 loudspeakers, $r_0 = 1.5$ m). Local WFS was used in (a) and (b) whereas the conventional WFS was used in (c) and (d). For local WFS, the local area is centered at $(0.75, 0, 0)$ with a radius of 0.3 m which is indicated by dashed circles. The driving functions were computed from the spherical harmonics expansion with the maximum order of $\mathcal{N} = 22$.

The driving function (22) depends on \mathbf{x} , and the synthesized sound field is accurate only at \mathbf{x} . This is a well-known property of 2.5D SFS, which is attributed to the mismatch of the sound field (2D) and the secondary source distribution (3D). The driving function is typically computed for a reference point which is, in this case, obviously the center of the local listening area $\mathbf{x} = \mathbf{0}$. The driving function thus reads

$$D_{2.5D}(\mathbf{x}_0, \omega) = \sqrt{\frac{2\pi\rho_0}{i\frac{\omega}{c}}} D_{2D}(\mathbf{x}_0, \omega). \quad (23)$$

Note that the additional term corrects the ampli-

tude decay and compensates the low-pass characteristic of the secondary line sources.

2.7 2.5D Driving Function II – $\check{S}_n^m(\omega)$

Another type of 2.5D WFS is considered where $S(\mathbf{x}, \omega)$ is represented by a spherical harmonics expansion but the secondary sources have a 2D distribution, e.g. linear or circular array. While the virtual sound field exhibits 3D properties, only a 2D sound field can be synthesized. It is thus convenient to convert the spherical harmonics expansion into a circular harmonics expansion. This process reduces one dimension of the sound field, and thus the conversion is non-invertible. One possibility

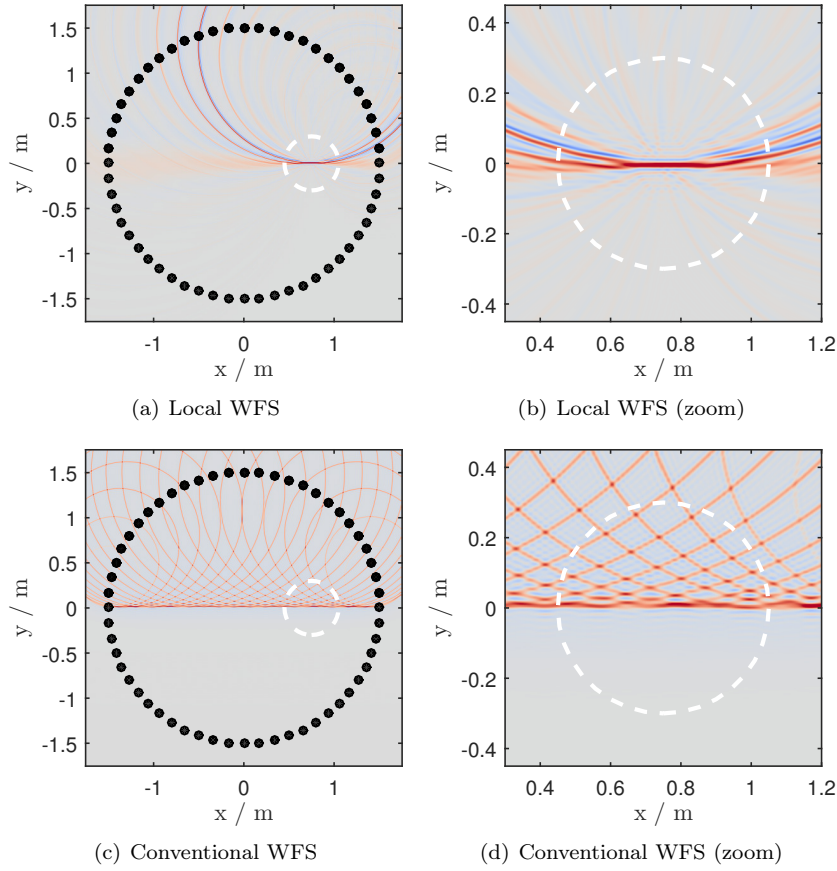


Fig. 3: Virtual plane waves ($\phi_{\text{PW}} = -\frac{\pi}{2}$) synthesized by using a circular loudspeaker array (56 loudspeakers, radius of $r_0 = 1.5$ m). Local WFS was used in (a) and (b) whereas the conventional WFS was used in (c) and (d). The local listening area is centered at $(0.75, 0, 0)$ with radius of 0.3 m which is indicated by dashed circles. The driving functions were computed from the circular harmonics expansion where the expansion order depends on the frequency $\mathcal{N}(f) = \lceil \frac{2\pi f}{c} R_l \rceil$. The maximum order was 122 for $f = fs/2$.

is to project the sound field onto the horizontal plane, as suggested in [13]. In this paper, only the horizontal slice of the virtual sound field is synthesized, i.e. $S(\mathbf{x}, \omega)|_{z=0}$.

In order to convert $\check{S}_n^m(\omega)$ to $\hat{S}_\mu^m(\omega)$, the order of summation in (5) is exchanged,

$$\sum_{m=-\infty}^{\infty} \left(\sum_{n=|m|}^{\infty} \check{S}_n^m(\omega) j_n\left(\frac{\omega}{c} r\right) Y_n^m(\theta, 0) \right) e^{im\phi} \quad (28)$$

where $Y_n^m(\theta, \phi) = Y_n^m(\theta, 0)e^{im\phi}$ is exploited. Com-

paring (28) with (4) on the xy -plane ($\theta = \frac{\pi}{2}$) yields

$$\sum_{n=|m|}^{\infty} \check{S}_n^m(\omega) j_n\left(\frac{\omega}{c} r\right) Y_n^m(\theta, 0) = \hat{S}_m^m J_m\left(\frac{\omega}{c} r\right) \quad (29)$$

where ρ is substituted by r . As shown in [20, Eq. (13)], the Bessel function can be represented as a weighted sum of spherical Bessel functions,

$$J_m\left(\frac{\omega}{c} r\right) = \sum_{n=|m|}^{\infty} 4\pi i^{m-n} Y_n^{-m}\left(\frac{\pi}{2}, 0\right) j_n\left(\frac{\omega}{c} r\right) Y_n^m\left(\frac{\pi}{2}, 0\right), \quad (30)$$

Driving functions	Section
$D_{2D}(\mathbf{x}_0, \omega) = -2a(\mathbf{x}_0) \sum_{\mu=-\mathcal{N}}^{\mathcal{N}} \check{S}_{\mu}(\omega) e^{i\mu\varphi_0}$ $\times \left[\langle \hat{\mathbf{e}}_r, \mathbf{n}_0 \rangle \frac{\omega}{2c} \left\{ J_{\mu-1}\left(\frac{\omega}{c}\rho_0\right) - J_{\mu+1}\left(\frac{\omega}{c}\rho_0\right) \right\} \right.$ $\left. + \langle \hat{\mathbf{e}}_{\varphi}, \mathbf{n}_0 \rangle i\mu J_{\mu}\left(\frac{\omega}{c}\rho_0\right) \right]$	2.4
$D_{3D}(\mathbf{x}_0, \omega) = -2a(\mathbf{x}_0) \sum_{n=0}^{\mathcal{N}} \sum_{m=-n}^n \check{S}_n^m(\omega)$ $\left[\langle \hat{\mathbf{e}}_r, \mathbf{n}_0 \rangle \frac{1}{2n+1} \frac{\omega}{c} \left\{ nj_{n-1}\left(\frac{\omega}{c}r_0\right) - (n+1)j_{n+1}\left(\frac{\omega}{c}r_0\right) \right\} Y_n^m(\theta_0, \phi_0) \right.$ $+ \langle \hat{\mathbf{e}}_{\theta}, \mathbf{n}_0 \rangle \frac{-1}{r_0 \sin^2 \theta_0} j_n\left(\frac{\omega}{c}r_0\right) \left\{ (n+1) \cos \theta_0 Y_n^m(\theta_0, \phi_0) \right.$ $\left. - \sqrt{\frac{2n+1}{2n+3}} \left((n+1)^2 - m^2 \right) Y_{n+1}^m(\theta_0, \phi_0) \right\}$ $\left. + \langle \hat{\mathbf{e}}_{\phi}, \mathbf{n}_0 \rangle \frac{im}{r_0 \sin \theta_0} j_n\left(\frac{\omega}{c}r_0\right) Y_n^m(\theta_0, \phi_0) \right]$	2.5
$D_{2.5D}(\mathbf{x}_0, \omega) = \sqrt{\frac{2\pi \ \mathbf{x} - \mathbf{x}_0\ }{i\frac{\omega}{c}}} \times D_{2D}(\mathbf{x}_0, \omega)$	2.6
$D_{2.5D}(\mathbf{x}_0, \omega) = -2a(\mathbf{x}_0) \sum_{m=-\mathcal{N}}^{\mathcal{N}} \frac{\check{S}_{ m }^m(\omega) e^{im\varphi_0}}{4\pi i^{ m -m} Y_{ m }^{-m}\left(\frac{\pi}{2}, 0\right)}$ $\times \left[\langle \hat{\mathbf{e}}_r, \mathbf{n}_0 \rangle \frac{\omega}{2c} \left\{ J_{m-1}\left(\frac{\omega}{c}\rho_0\right) - J_{m+1}\left(\frac{\omega}{c}\rho_0\right) \right\} \right.$ $\left. + \langle \hat{\mathbf{e}}_{\varphi}, \mathbf{n}_0 \rangle im J_m\left(\frac{\omega}{c}\rho_0\right) \right]$	2.7

Table 1: WFS driving functions derived from circular/spherical harmonics expansions.

and thus

$$\check{S}_m(\omega) = \frac{\sum_{n=|m|}^{\infty} \check{S}_n^m(\omega) j_n\left(\frac{\omega}{c}r\right) Y_n^m\left(\frac{\pi}{2}, 0\right)}{\sum_{n=|m|}^{\infty} 4\pi i^{m-n} Y_n^{-m}\left(\frac{\pi}{2}, 0\right) j_n\left(\frac{\omega}{c}r\right) Y_n^m\left(\frac{\pi}{2}, 0\right)}. \quad (31)$$

The conversion of the coefficients is only valid for a distinct radius r and θ . Thus, the sound pressures of the spherically and the cylindrically expanded sound fields do only coincide at that coordinate. Choosing the origin and applying the

rule of l'Hospital results in

$$\check{S}_m(\omega) = \frac{\check{S}_{|m|}^m(\omega)}{4\pi i^{m-|m|} Y_{|m|}^{-m}\left(\frac{\pi}{2}, 0\right)}. \quad (32)$$

The 2.5D driving function can be computed by substituting (32) into (26) (see Table 1). The resulting driving function (27) is listed in Table 1.

Note that the driving function only requires a subset of $\check{S}_n^m(\omega)$ where $n = |m|$. Not surprisingly, NFC-HOA also uses the same coefficients for 2.5D synthesis using a circular array [4, Eq. (20)].

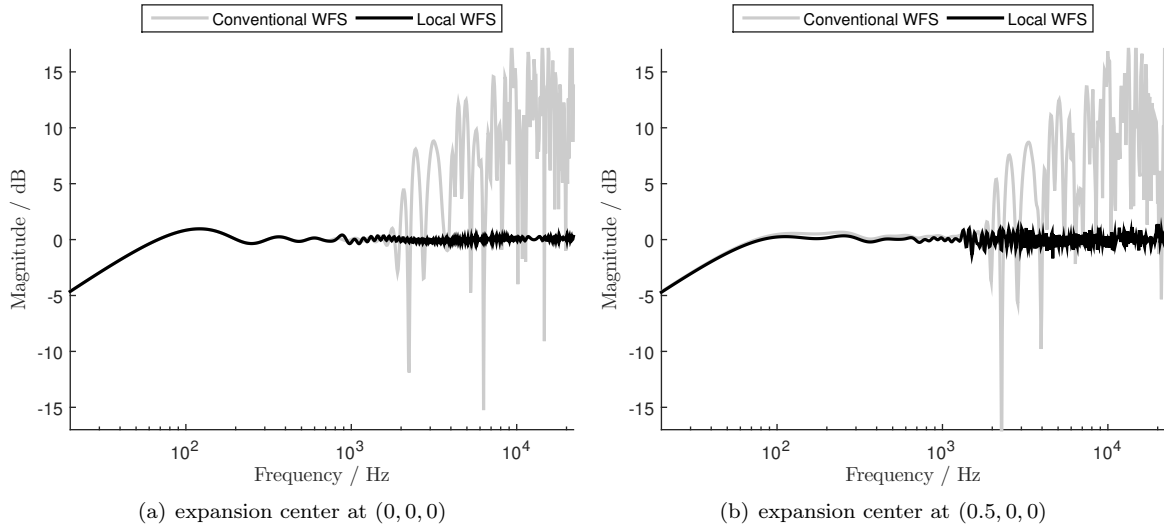


Fig. 4: Frequency responses of a broadband plane wave ($\phi_{PW} = -\frac{\pi}{2}$) synthesized by a circular loudspeaker array (56 loudspeakers, $r_0 = 1.5$ m). For local WFS, the local area ($R_l = 0.3$ m) in (a) and (b) are centered at $(0, 0, 0)$ and $(0.5, 0, 0)$, respectively. The driving functions were computed from the circular harmonics expansion with a fixed order $\mathcal{N} = 22$.

3 Evaluation

The driving functions derived in the previous section are used in numerical simulations of various scenarios. Only 2.5D WFS is considered where either a circular or rectangular array is used. The circular array consists of 56 loudspeakers as the system installed in the Technical University of Berlin. The rectangular array with 64 loudspeakers is identical to the system installed in the University of Rostock [21]. The loudspeakers are assumed to be monopole point sources. Free-field sound propagation was considered and the speed of sound was set to 343 m/s. The sampling frequency was $f_s = 44.1$ kHz. All simulation results were obtained by the Sound Field Synthesis Toolbox ver. 2.1.0 [22].

The advantage of local WFS compared to (non-local) WFS is demonstrated in Fig. 2. A monochromatic sound field of a point source is synthesized where the frequency (4 kHz) is well above the spatial aliasing frequency (≈ 1 kHz) of the system. The driving functions are computed by using (27) together with the spherical harmonics expansion coefficients of a point source,

$$\check{S}_n^m(\omega) = -i \frac{\omega}{c} h_n^{(2)}\left(\frac{\omega}{c} r_{PS}\right) Y_n^{-m}(\theta_{PS}, \phi_{PS}) \quad (33)$$

where $(r_{PS}, \theta_{PS}, \phi_{PS})$ is the spherical coordinates of the source position. The reproduced sound field for conventional WFS suffers from strong artifacts regardless of the listening position. In local WFS, on the other hand, the sound field within the local listening area (dashed circle) exhibits a better spatial structure. The amplitude is more evenly distributed and also the phase is correctly synthesized.

In Fig. 3, a broadband plane wave is synthesized carrying a Dirac shaped signal. The driving function is computed for discrete frequencies and transformed to the time domain by inverse Fourier transform. In conventional WFS, shown in Fig. 3(c) and 3(d), the first wavefront is perfectly synthesized but it is followed by multiple wavefronts arriving from different directions. In local WFS, a sharp wavefront is observed in the middle of the local area. Interestingly, the sound field in Fig. 3(a) looks very similar to the sound field synthesized by NFC-HOA [23, Fig. 1(c)] except the spatial shift by $(0.5, 0, 0)$. This is not surprising because both in NFC-HOA and local WFS, spatial band-limitation is applied to the target sound field. This representation of the sound field seems to have a strong influence on the synthesized sound field.

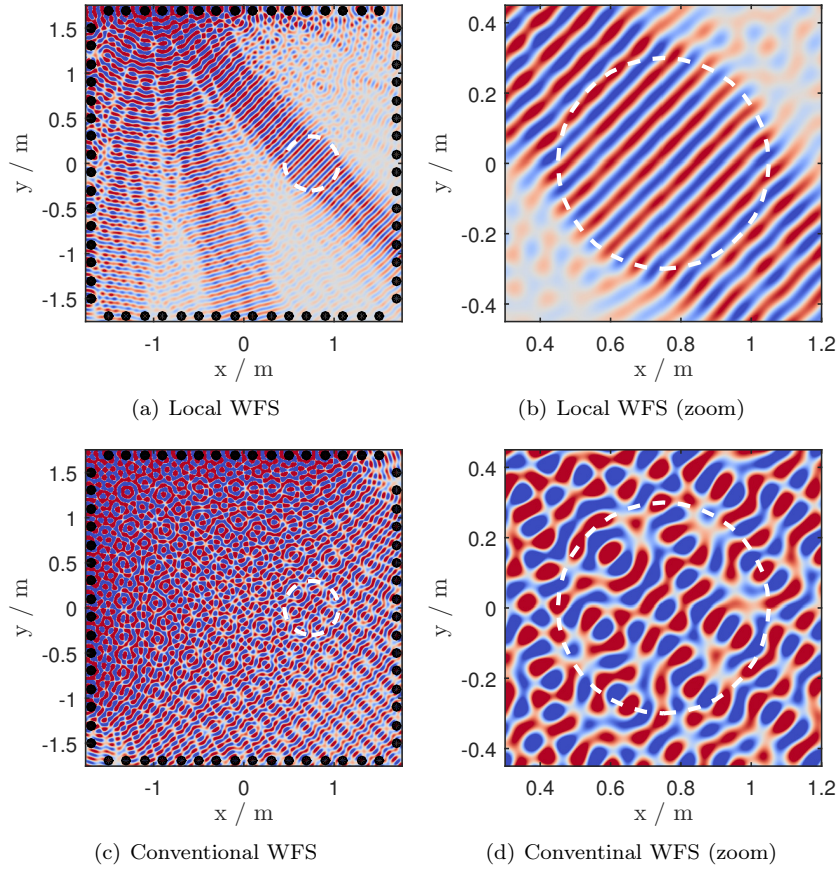


Fig. 5: Virtual plane wave ($\phi_{\text{PW}} = -\frac{\pi}{4}$, $f = 4$ kHz) synthesized by local WFS and conventional WFS using a rectangular loudspeaker array (64 loudspeakers). Local WFS was used in (a) and (b) whereas the conventional WFS was used in (c) and (d). The local listening area is indicated by dashed circles centered at $(0.75, 0, 0)$ with a radius of 0.3 m. The driving functions were computed from the spherical harmonics expansion with maximum order of $\mathcal{N} = 22$.

The frequency responses for different listening positions are shown in Fig. 4. Two different local listening areas centered at $(0, 0, 0)$ and $(0.5, 0, 0)$ are considered. The radius of the listening area is 0.3 m in both cases. Below the aliasing frequency (≈ 1 kHz) the magnitude responses are almost identical, but at high frequencies the advantage of local WFS is clearly visible. In conventional WFS, spatial aliasing adds more energy in high frequencies thereby resulting in a high-pass characteristic. Due to the strong fluctuation, only an approximate equalization is possible. In typical WFS systems, a pre-equalization filter is applied to the input signal [24]. Local WFS, on the other hand, exhibits better spectral properties.

The fluctuation is in the order of ± 1 dB. Both for conventional and local WFS, a low-pass characteristic is observed below 100 Hz which is attributed to the high-frequency assumption in the derivation of WFS.

WFS can be applied for arbitrary secondary source distributions. In Fig. 5, a monochromatic sound field is synthesized by using a rectangular array. The advantage of local WFS is clearly observable.

4 Conclusion

A new approach for local WFS is presented in this paper. It is based on the representation of

the virtual sound field by a band-limited circular/spherical harmonics expansion. Due to the property of spatial band-limitation, the sound field within a local region can be synthesized with higher precision than conventional WFS. Local WFS driving functions are derived for 2D, 2.5D and 3D WFS as summarized in Table 1. Two variations of 2.5D WFS driving functions are presented where circular and spherical harmonics representations are considered, respectively.

As demonstrated by numerical simulations, the local SFS method improves the technical performance inside a predetermined target region. Therefore, local SFS can be applied where the listener(s) can be assumed to be in a fixed region or if the listener position can be estimated by a tracking system. The achievable perceptual improvement, however, is still under investigation. The comparison between different local SFS methods is an open topic and will be addressed in following studies.

References

- [1] Berkhout, A. J., de Vries, D., and Vogel, P., "Acoustic Control by Wave Field Synthesis," *The Journal of the Acoustical Society of America (JASA)*, 93(5), pp. 2764–2778, 1993.
- [2] Spors, S., Rabenstein, R., and Ahrens, J., "The Theory of Wave Field Synthesis Revisited," in *Proc. of 124th Audio Engineering Society (AES) Convention*, pp. 17–20, 2008.
- [3] Daniel, J., Moreau, S., and Nicol, R., "Further Investigations of High-order Ambisonics and Wavefield Synthesis for Holophonic Sound Imaging," in *Proc. of 114th Audio Engineering Society (AES) Convention*, 2003.
- [4] Ahrens, J. and Spors, S., "An Analytical Approach to Sound Field Reproduction Using Circular and Spherical Loudspeaker Distributions," *Acta Acustica united with Acustica*, 94(6), pp. 988–999, 2008.
- [5] Spors, S. and Rabenstein, R., "Spatial Aliasing Artifacts Produced by Linear and Circular Loudspeaker Arrays used for Wave Field Synthesis," in *Proc. of 120th Audio Engineering Society (AES) Convention*, Paris, France, 2006.
- [6] Wu, Y. J. and Abhayapala, T. D., "Spatial Multizone Soundfield Reproduction," in *Proc. of International Conference on Acoustics, Speech and Signal Processing (ICASSP)*, pp. 93–96, IEEE, 2009.
- [7] Ahrens, J. and Spors, S., "An Analytical Approach to Sound Field Reproduction with a Movable Sweet Spot using Circular Distributions of Loudspeakers," in *Proc. of International Conference on Acoustics, Speech and Signal Processing (ICASSP)*, Taipei, Taiwan, 2009.
- [8] Spors, S. and Ahrens, J., "Local Sound Field Synthesis by Virtual Secondary Sources," in *Proc. of 40th Audio Engineering Society (AES) International Conference on Spatial Audio*, Tokyo, Japan, 2010, ISBN 978-0-937803-77-6.
- [9] Spors, S., Helwani, K., and Ahrens, J., "Local Sound Field Synthesis by Virtual Acoustic Scattering and Time-reversal," in *Proc. of 131st Audio Engineering Society (AES) Convention*, Audio Engineering Society (AES), New York, USA, 2011.
- [10] Winter, F., Ahrens, J., and Spors, S., "On Analytic Methods for 2.5 D Local Sound Field Synthesis Using Circular Distributions of Secondary Sources," *IEEE Transactions on Speech and Audio Processing*, pp. 914–926, 2016.
- [11] Fazi, F. M., *Sound field reproduction*, Ph.D. thesis, University of Southampton, 2010.
- [12] Spors, S., "Extension of an Analytic Secondary Source Selection Criterion for Wave Field Synthesis," in *Proc. of 123rd Audio Engineering Society (AES) Convention*, New York, USA, 2007.
- [13] Ahrens, J. and Spors, S., "Wave Field Synthesis of a Sound Field Described by Spherical Harmonics Expansion Coefficients," *Journal of the Acoustical Society of America (JASA)*, 131(3), pp. 2190–2199, 2012, doi:10.1121/1.3682036.

- [14] Fazi, F. M., Olivieri, F., Carpentier, T., and Noisternig, M., “Wave Field Synthesis of Virtual Sound Sources with Axisymmetric Radiation Pattern Using a Planar Loudspeaker Array,” in *Proc. of 134th Audio Engineering Society (AES) Convention*, Audio Engineering Society, 2013.
- [15] Ahrens, J. and Spors, S., “Implementation of Directional Sources in Wave Field Synthesis,” in *Proc. of Workshop on Applications of Signal Processing to Audio and Acoustics (WASPAA)*, IEEE, New Paltz, USA, 2007.
- [16] Corteel, E., “Synthesis of Directional Sources using Wave Field Synthesis, Possibilities, and Limitations,” *EURASIP Journal on Advances in Signal Processing*, 2007(1), pp. 1–18, 2007.
- [17] Williams, E. G., *Fourier Acoustics: Sound Radiation and Nearfield Acoustical Holography*, Academic Press, 1999.
- [18] Kennedy, R. A., Sadeghi, P., Abhayapala, T. D., and Jones, H. M., “Intrinsic Limits of Dimensionality and Richness in Random Multipath Fields,” *IEEE Transactions on Signal Processing*, 55(6), pp. 2542–2556, 2007.
- [19] Abramowitz, M. and Stegun, I. A., *Handbook of Mathematical Functions: with Formulas, Graphs, and Mathematical Tables*, 55, Courier Dover Publications, 1972.
- [20] Hahn, N. and Spors, S., “Sound Field Synthesis of Virtual Cylindrical Waves using Circular and Spherical Loudspeaker Arrays,” in *Proc. of 138th Audio Engineering Society (AES) Convention*, Warsaw, Poland, 2015.
- [21] Erbes, V., Geier, M., Weinzierl, S., and Spors, S., “Database of Single-channel and Binaural Room Impulse Responses of a 64-channel Loudspeaker Array,” in *Proc. of 138th Audio Engineering Society (AES) Convention*, Warsaw, Poland, 2015.
- [22] Wierstorf, H. and Spors, S., “Sound Field Synthesis Toolbox,” in *Proc. of 132nd Audio Engineering Society (AES) Convention*, 2012.
- [23] Ahrens, J., Spors, S., and Wierstorf, H., “Comparison of Higher Order Ambisonics and Wave Field Synthesis with respect to Spatial Discretization Artifacts in Time Domain,” in *Proc. of 40th Audio Engineering Society (AES) International Conference on Spatial Audio*, 2010.
- [24] Spors, S. and Ahrens, J., “Analysis and Improvement of Pre-equalization in 2.5-dimensional Wave Field Synthesis,” in *Proc. of 128th Audio Engineering Society (AES) Convention*, London, UK, 2010, ISBN 978-0-937803-74-5.